Laser-excited fluorescence and electron-spin resonance of Er^{3+} in polycrystalline $AlCl_3$

G. Ceotto, M. A. Pires, J. A. Sanjurjo, C. Rettori, and G. E. Barberis

Instituto de Física, Universidade Estadual de Campinas, 13081 Campinas, São Paulo, Brazil

(Received 19 July 1989)

The green fluorescence transitions among the levels corresponding to the $^4S_{3/2}$ and $^4I_{15/2}$ configurations of Er^{3+} diluted in $AlCl_3$ have been measured using laser excitation. The data allow us to determine the crystalline-field splittings of these levels and, in turn, the spin-Hamiltonian parameters. The electron-paramagnetic-resonance spectrum observed at low temperatures is in good agreement with that expected from these parameters.

I. INTRODUCTION

Recently, much interest in the behavior of $AlCl_3$ graphite intercalation compounds (GiC's) has arisen, and several techniques were used to study these materials.[1-5] Electron-spin-resonance (ESR) studies[2-5] of these highly anisotropic layered compounds focused mainly on the resonance of conduction electrons[2-4] and the resonances of Mn^{2+} ions[5] introduced as impurities in the intercalant $AlCl_3$.

In order to understand the local environment of rare-earth impurities in $AlCl_3$ GIC's, we first need to study the behavior of the rare-earth impurities in $AlCl_3$. The basic features of rare-earth impurities in transparent solids is today well understood,[6] particularly the Er^{3+} ion in several crystal-field environments.[7,8] Optical experiments allow one to obtain the crystal-field parameters, and complementary ESR experiments can be used to confirm them. Er^{3+} in crystalline YCl_3, which is isomorphous to $AlCl_3$, was studied by optical techniques[9] and also by ESR (Ref. 10) long ago. Surprisingly enough, we were not able to find similar studies in $R^{3+}:AlCl_3$ (where R is any rare-earth) which could be referred to. Therefore, we decided to report the initial results of our study.

The present work then consists of an optical and ESR study of the $Er^{3+}:AlCl_3$ system. The obtained knowledge will be important for our work in progress in the corresponding GIC's.

II. EXPERIMENTAL DETAILS

$AlCl_3$ and $ErCl_3$ are isomorphous compounds; however, they melt at very different temperatures (192.4 and 774.0 °C, respectively). This makes the matter of sample preparation a problem of great difficulty. In order to prepare our samples, we made an alloy of $Al_{0.9}Er_{0.1}$ by arc melting the pure components in an argon atmosphere. The alloy was then powdered and inserted into a quartz tube connected to a Cl_2 reactor with controlled pressure. Heating the powder with a flame, a large amount of polycrystalline salt was formed. Since the salt is very hygroscopic, the product of the reaction was sealed in He atmosphere into a quartz ampoule, suited both for the ESR and fluorescence experiments.

The fluorescence spectrum was excited with an argon-ion laser using the 4880 and 4765 Å lines. The quartz ampoule containing the polycrystalline sample was at-tached to the cold finger of a closed-cycle helium refrigerator. To avoid the heating of the sample by the incident light, the laser power was kept below 10 mW. The light emitted by the sample was analyzed using a Spex 1401 double monochromator. The radiation was detected by an RCA 31034 photomultiplier and standard photon-counting electronics. The fluorescence lines are determined within 1 cm^{-1} accuracy and the spectral resolution was about 0.5 cm^{-1}.

The ESR measurements were carried out using a Varian E-line standard X-band spectrometer. As usual, 100-KHz modulation and field sweep were used in the experiment. Two different systems were used in order to obtain the required temperatures of the sample. For temperatures below 4.2 K the samples were immersed in liquid ^{4}He using a quartz tail Dewar which was inserted in a room-temperature TE_{102} cavity. The liquid ^{4}He was pumped and the vapor pressure measured in order to determine the temperature of the sample. For the high-temperature range, a ^{4}He flux system (Air Products) inserted in the same cavity was used. Three thermocouples were used to control and measure the temperature of the sample.

III. RESULTS AND ANALYSIS

$AlCl_3$ crystallizes in the monoclinic (almost hexagonal) structure with space group $C2/m$ (C_{2h}^3). The lattice parameters are $a = 5.92$, $b = 10.22$, and $c = 6.16$ Å with an angle of 108° between the a-b plane and the c axis. The Al atoms occupy $(4g)$ positions, with coordinates $\pm(0,u,0)$ and $\pm(\frac{1}{2},u+\frac{1}{2},0)$ with $u = 0.167$; the Cl(1) occupy $(4i)$ positions, with coordinates $\pm(u,0,v)$ and $\pm(u+\frac{1}{2},\frac{1}{2},v)$ with $u = 0.226$ and $v = 0.219$, and the Cl(2) occupy $(8j)$ positions with coordinates $\pm(x,y,z)$; $\pm(x,-y,z)$; $\pm(x+\frac{1}{2},y+\frac{1}{2},z)$; and $\pm(x+\frac{1}{2},\frac{1}{2}-y,z)$ with $x = 0.250$, $y = 0.175$, and $z = -0.219$.[8] The RCl_3 salts for the second half of the rare-earth series, crystallize isostructurally with $AlCl_3$.[11] This means that, as an impurity, Er substitutes for Al. The point symmetry of Al (or Er) in the $AlCl_3$ crystal is nearly octahedral,[9] with small distortions reducing the point group to C_2.

Figures 1 and 2 show the observed upper and lower groups of fluorescence transitions between the $^4S_{3/2}$ and $^4I_{15/2}$ configurations of Er^{3+} in $AlCl_3$ at temperatures of about 15 K. Both groups are separated by a gap of about 210 cm^{-1} which is characteristic of this crystal structure,
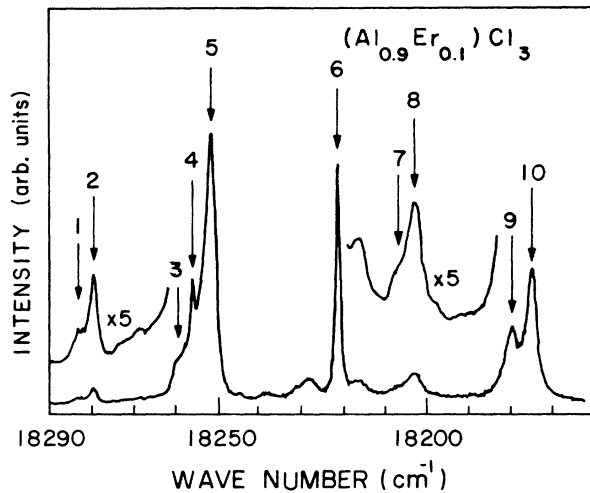
FIG. 1. Er^{3+}: $AlCl_3$ fluorescence spectra (higher-energy region). The labels on the lines correspond with the level scheme in Fig. 3 and Table I. The indicated composition is the nominal one (see text).

and also observed in the isomorphous YCl_3 host.[9] The crystal-field transitions were identified using published data for Er^{3+} in different crystalline hosts and also following the temperature dependence of their relative intensity. These transitions are labeled in Figs. 1–3 and the corresponding energies are listed in Table I. These figures also show several other lines of weaker intensity, which are probably due to phonon sidebands and impurity-induced satellites.[12] It has been shown in several hosts that for Er^{3+} concentrations higher than 1 mol%, due to a nonresonant cross-relaxation process between Er^{3+}-Er^{3+} pairs, the red-emission fluorescence ($^4F_{9/2} \rightarrow ^4I_{15/2}$) predominates over the green one.[13] We have also measured this red emission at 15 K. We found that the overall intensity of this transition is much smaller than for the green one. Therefore, we conclude that the Er^{3+} concentration in our samples should be much lower than that ex-
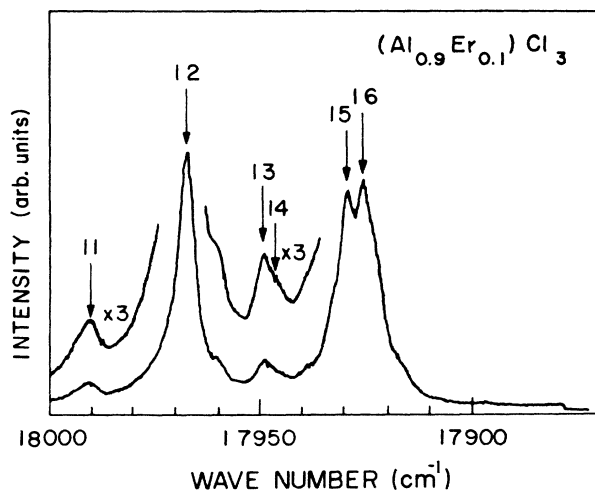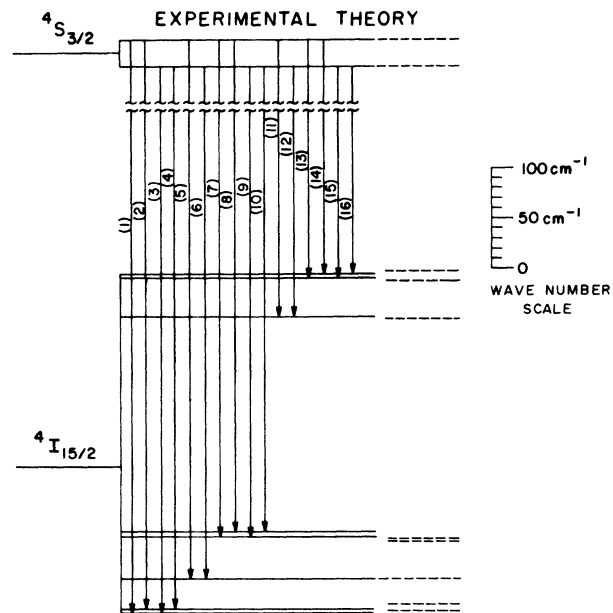

FIG. 3. Theoretical and experimental level scheme of Er^{3+}: $AlCl_3$ as obtained from the fluorescence spectra and the least-squares fitting of Eq. (1) to the optical data.

pected from the nominal concentration of our alloys.

ESR experiments on our samples show a single resonance line at a g value of about 8.90. As we discuss below, this resonance corresponds to the first excited Kramers' doublet of the crystal-field split Γ_8. The resonance corresponding to the ground-state Kramers' doublet is not observed, suggesting large g value and/or linewidth anisotropy for this doublet.

In order to obtain the crystal-field parameters of Er^{3+} in $AlCl_3$, we write a spin-Hamiltonian operating on the $^4I_{15/2}$ term, incorporating a trigonal distortion and a cubic

FIG. 2. Lower-energy region of Er^{3+}:$AlCl_3$ fluorescence spectra. The labels are as in Fig. 1.

TABLE I. The fluorescence transitions of Er^{3+}: $AlCl_3$ at 15 K.

| Label	Wavelength (Å)	E/hc (cm^{-1})	Transition
1	5469.6	18 283	$S_{3/2},2 \rightarrow I_{15/2},1$
2	5471.0	18 279	$S_{3/2},2 \rightarrow I_{15/2},2$
3	5476.6	18 259	$S_{3/2},1 \rightarrow I_{15/2},1$
4	5477.7	18 256	$S_{3/2},1 \rightarrow I_{15/2},2$
5	5479.1	18 251	$S_{3/2},2 \rightarrow I_{15/2},3$
6	5488.1	18 221	$S_{3/2},1 \rightarrow I_{15/2},3$
7	5492.1	18 208	$S_{3/2},2 \rightarrow I_{15/2},4$
8	5493.6	18 203	$S_{3/2},2 \rightarrow I_{15/2},5$
9	5500.7	18 179	$S_{3/2},1 \rightarrow I_{15/2},4$
10	5502.1	18 175	$S_{3/2},1 \rightarrow I_{15/2},5$
11	5558.5	17 991	$S_{3/2},2 \rightarrow I_{15/2},6$
12	5565.8	17 967	$S_{3/2},1 \rightarrow I_{15/2},6$
13	5571.4	17 949	$S_{3/2},2 \rightarrow I_{15/2},7$
14	5572.3	17 946	$S_{3/2},2 \rightarrow I_{15/2},8$
15	5577.6	17 929	$S_{3/2},1 \rightarrow I_{15/2},7$
16	5578.7	17 925	$S_{3/2},1 \rightarrow I_{15/2},8$
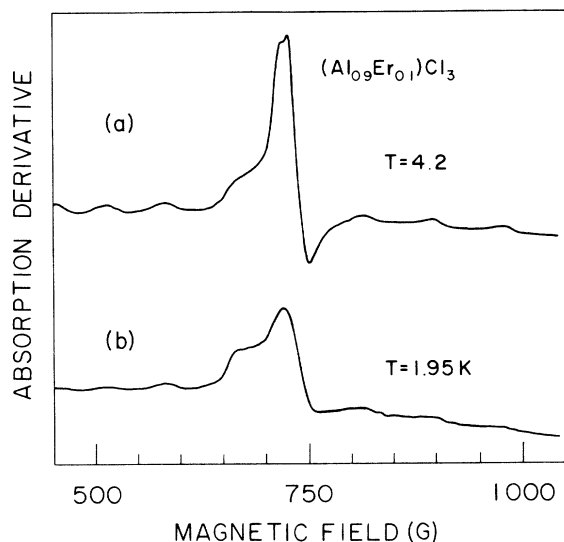
FIG. 4. ESR spectra of Er^{3+}: $AlCl_3$ at two different temperatures. The resonance corresponds to an excited Kramers' doublet (see text).

crystal field. The Hamiltonian can be written as follows:

$$\hat{\mathcal{H}} = B_2[O_2^1(c) + O_2^1(s) + O_2^2(s)] + B_4[O_4^0(c) + 5O_4^4(c)]$$

$$+ B_6[O_6^0(c) - 21O_6^4(c)] ,$$ (1)

where the first term on the right-hand side of Eq. (1) represents the trigonal distortion and the second and third terms are the cubic crystal field. As usual, the $O_n^m(c)$ and $O_n^m(s)$ are Stevens' operators transforming as the real combinations of spherical harmonics C_n^m and S_n^m tabulated by Prather,[14] and where the $O_n^0(c)$ are normalized following Hutchings.[15] A small second-order term representing a tetragonal distortion also has been added to the Hamiltonian in Eq. (1), but the value obtained for this parameter is of the order of the experimental error. Diagonalizing the whole 16×16 matrix of the Hamiltonian, and using a least-squares program developed for nonlinear regression, we obtain from the best fit of the optical data the following crystal-field parameters (in cm^{-1}):

$$B_2/(hc) = (1.04 \pm 0.05) \times 10^{-1} ,$$

$$B_4/(hc) = (9.11 \pm 0.09) \times 10^{-3} ,$$

$$B_6/(hc) = (2.24 \pm 0.07) \times 10^{-5} .$$

Figure 3 shows the observed optical transitions and the calculated levels corresponding to these parameters. The g values of the first excited Kramers' doublet calculated with these parameters yield $g_{\parallel} = 8.77$ and $g_{\perp} = 1.22$. The parallel g value is in reasonable agreement with the experimental result ($g = 8.9 \pm 0.2$).

Figure 4 shows the ESR spectra at two different temperatures. The line shape is characteristic of the powder spectrum for an anisotropic g tensor. The spectra show the completely resolved hyperfine lines for the ^{167}Er ($I = \frac{7}{2}$, 22.9%) isotope, with the appropriate value of the hyperfine parameter $A = (74 \pm 2)$ G. The intensity of the resonance as a function of temperature is plotted in Fig. 5.
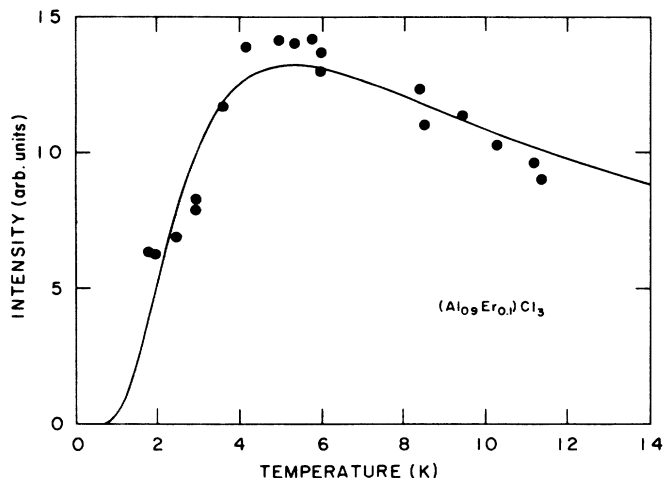

FIG. 5. ESR intensities vs temperature. The solid line shows the best fit of Eq. (2) to the experiments.

The solid line represents the least-squares fitting of the ESR intensity to the Boltzmann thermal population distribution given by

$$I(T) = \{\exp[-(E_1 - h\nu/2)/kT]$$

$$-\exp[-(E_1 + h\nu/2)/kT]\}/Z(T) ,$$ (2)

where the $Z(T)$ is the partition function

$$Z(T) = 2\sum_i e^{-E_i/kT} ,$$

E_i are the energies of the Kramers' doublets, and $h\nu$ the microwave energy. The intensities plotted in Fig. 5 were calculated by numerical integration of the resonances in order to minimize the errors coming from the fact that the lines are nonsymmetric. The best fitting gives $E_1 = 6.8 \pm 0.8$ K, which is in excellent agreement with the value obtained from the fluorescence data for the first excited Kramers' doublet (see Fig. 3).

IV. CONCLUSIONS

In summary, we obtained the crystal-field parameters by fitting the experimental fluorescence lines in Er^{3+}: $AlCl_3$. These parameters allowed us to calculate the wave functions corresponding to the lower Er^{3+} multiplet, and in turn the g value and the energy position of the excited doublet responsible for the observed resonance. These values agree very well with the experimental ESR data. We believe that this work completes ESR and fluorescence data reported in isomorphous compounds.

ACKNOWLEDGMENTS

[1]G. M. Gualberto, C. Underhill, S. Y. Leung, and G. Dresselhaus, Phys. Rev. B **21**, 862 (1980).

[2]R. M. Stein, L. Walmsley, G. M. Gualberto, and C. Rettori, Phys. Rev. B **22**, 4774 (1985).

[3]R. M. Stein, L. Walmsley, S. Rolla, and C. Rettori, Synth. Met. **12**, 407 (1985).

[4]S. Rolla, L. C. Walmsley, and C. Rettori, Synth. Met. **23**, 43 (1988).

[5]G. Ceotto, S. Rolla, G. E. Barberis, and C. Rettori, in *Graphite Intercalation Compounds, Extended Abstracts,* edited by M. S. Dresselhaus, G. Dresselhaus, and S. A. Solin (Materials Research Society, Pittsburgh, 1986), p. 187.

[6]S. Hüfner, in *Optical Spectra of Transparent Rare Earth Compounds* (Academic, New York, 1967).

[7]H. M. Crosswhite and H. W. Moos, in *Optical Properties of Ions in Crystals,* edited by H. M. Crosswhite and H. W. Moos (Interscience, New York, 1967), p. 3.

[8]C. A. Hutchinson, Jr., S. G. Utterback, and P. M. Martineau, Phys. Rev. B **39**, 4051 (1989).

[9]J. W. Rakestraw and G. H. Dieke, J. Chem. Phys. **42**, 873 (1965), and references therein.

[10]G. Garton, M. T. Hutchings, R. Shore, and W. P. Wolf, J. Chem. Phys. **41**, 1970 (1964).

[11]R. W. G. Wyckoft, *Crystal Structures* (Interscience, New York, 1949).

[12]E. Cohen, L. A. Riseberg, and H. W. Moos, Phys. Rev. **175**, 521 (1968).

[13]J. P. Jouart and G. P. Mary, Phys. Status Solidi (b) **149**, 633 (1988).

[14]J. L. Prather, U.S. National Bureau of Standards Monograph No. 19 (U.S. GPO, Washington, DC, 1961).

[15]M. T. Hutchings, in *Solid State Physics,* edited by H. Ehrenreich, F. Seitz, and D. Turnbull (Academic, New York, 1964), Vol. 16, p. 227.